

# Unconventional p-wave magnets

Anna Birk Hellenes,<sup>1</sup> Tomáš Jungwirth,<sup>2,3</sup> Jairo Sinova,<sup>1,2</sup> and Libor Šmejkal<sup>1,2</sup>

<sup>1</sup>*Institut für Physik, Johannes Gutenberg Universität Mainz, D-55099 Mainz, Germany*

<sup>2</sup>*Institute of Physics, Czech Academy of Sciences, Cukrovarnická 10, 162 00, Praha 6, Czech Republic*

<sup>3</sup>*School of Physics and Astronomy, University of Nottingham, NG7 2RD, Nottingham, United Kingdom*  
(Dated: March 5, 2024)

The electronic structure of atoms is organized into even and odd-parity-wave s, p, d, ... orbitals. An analogous classification of condensed matter phases emerged with the discovery of conventional s-wave superconductivity in mercury, followed by the discoveries of unconventional p-wave superfluidity in <sup>3</sup>He and unconventional d-wave superconductivity in cuprates. To date, the known counterparts in magnetism have been the conventional ferromagnets with s-wave spin polarization in the electronic structure, and the recently discovered altermagnets [1–3] with unconventional d-wave and higher even-parity wave spin polarization [1, 2, 4–7]. Here we identify the long-sought magnetic counterpart of unconventional p-wave superfluidity [8, 9] – the unconventional magnet with p-wave spin polarization [10, 11]. We show that that collinear p-wave spin-polarization arises in a coplanar spin-symmetry subset of a class of noncentrosymmetric and noncolinear magnetic crystals with combined time-reversal and lattice translation symmetry. Contrary to common assumptions [12–15], we show that noncollinear magnets from this class universally exhibit nonrelativistic spin splittings and that these odd-parity wave spin splittings preserve time-reversal symmetry of the band structure. We predict large spin splittings reaching 500 meV by first-principles calculations and we identify 60 realistic material candidates. Inspired by the rich and anisotropic properties of superfluid <sup>3</sup>He [8, 9], our result opens up a wide range of possibilities to investigate unconventional p-wave order parameters in crystals and their exploitation in spintronics and topological physics [16–21].

## INTRODUCTION

Conventional spin-dependent electronic structures with time-reversal ( $\mathcal{T}$ ) symmetry are generated by the relativistic spin-orbit coupling term of the Dirac equation,  $\sim 1/c^2 \mathbf{s} \cdot (\mathbf{k} \times \mathbf{E})$  [22]. Here  $c$  is the speed of light,  $\mathbf{E}$  is electric field, and  $\mathbf{s}$  and  $\mathbf{k}$  are the electron spin and momentum. The relativistic spin-orbit coupling leads to numerous phenomena of fundamental and applied interest in areas including the spin Hall and other charge-spin conversion effects [16], topological insulators, or quantum computing [16–18, 20]. These phenomena are relevant usually in crystals with heavy and often toxic elements, because the magnitude of the spin-orbit coupling is limited by its perturbative ( $\sim 1/c^2$ ) relativistic nature and scales with a power of the atomic number [23].

Identifying alternative mechanisms for generating spin-dependent electronic structures with  $\mathcal{T}$  symmetry that do not require the strongly relativistic heavy elements has been a key open problem for decades [10, 11, 24]. The particularly appealing candidates are mechanisms based on the strong Coulomb interaction operating directly in the nonrelativistic limit of the Dirac equation without relying on the perturbatively weak  $\sim 1/c^2$  expansion. In magnetically-ordered systems, the Coulomb-exchange interaction was considered to enable such a mechanism [10, 11] in an envisioned unconventional p-wave magnetic phase. It could lead to a  $\mathcal{T}$ -symmetric electronic structure, characteristic of the relativistic spin-orbit coupling, but with potentially orders of magnitude larger

spin splittings and not relying on the presence of the relativistic heavy elements. However, a real physical realization of such an unconventional p-wave magnetic phase has been elusive. Moreover, in the context of Fermi-liquid instabilities in strongly correlated magnets, general principle obstacles have been identified that could prohibit the formation of a correlated p-wave magnetic phase [25, 26].

In contrast, even-parity wave (d, g, or i-wave) altermagnetism, has been recently predicted and classified in a range of materials by a spin-group formalism, designed to classify and describe magnetism from basic symmetry principles [1, 2]. Unlike the conventional relativistic magnetic groups tailored to the description of the full Dirac equation, the symmetry transformations in the nonrelativistic spin groups consider pairs of generally different operations acting on spin and lattice degrees of freedom.

The spin-group classification enabled to identify altermagnetic materials ranging from insulators to superconductors, to guide direct spectroscopic confirmation of their unconventional spin-dependent band structures both in relativistic [5, 6] and nonrelativistic limits [5–7], and to demonstrate their unconventional phenomenology, particularly in the field of spintronics [1, 2, 4, 27–35]. A characteristic feature of the even-parity wave altermagnets is the correspondence between the collinear ordering of magnetic density with alternating sign in the real-space crystal structure, and the collinear spin polarization with alternating sign and momentum-independent spin quantization axis in the

nonrelativistic band structure that breaks  $\mathcal{T}$  symmetry [1, 2, 4].

The realization of the nonrelativistic band structure with the d-wave (or higher even-parity wave) spin polarization in altermagnets prompts the question of whether a p-wave spin polarization in a  $\mathcal{T}$ -symmetric band structure can be identified in realistic material candidates starting also from the spin-symmetry considerations of the magnetic crystal structure.

In this manuscript we affirmatively answer the above question by demonstrating the unconventional p-wave magnetic counterpart of the superfluid  $^3\text{He}$ , starting from the spin-symmetry considerations and confirming it by first-principles calculations. Since odd-parity wave spin polarization is excluded by spin-symmetry in the nonrelativistic band structure of collinear magnets [1, 2], our focus is on crystal structures with a noncollinear magnetic order and corresponding noncollinear exchange fields. Remarkably, we demonstrate that a noncollinear coplanar magnetic order in the crystal can generate a collinear p-wave spin polarization in a  $\mathcal{T}$ -symmetric band structure with the momentum independent spin axis. In noncoplanar magnetic crystals we then demonstrate a  $\mathcal{T}$ -symmetric band structure with a momentum-dependent spin texture, representing the nonrelativistic unconventional magnetic counterpart of the conventional relativistic spin-orbit coupling.

### SPIN-SYMMETRY CLASSIFICATION OF UNCONVENTIONAL MAGNETISM

In this section, we formulate symmetry criteria for unconventional odd-parity wave magnets with nonrelativistic spin-split band structures. We first discuss the recent classification of collinear magnetic structures [1, 2]. The collinear magnets have a nonrelativistic spin symmetry consisting of arbitrary spin-space rotations  $C_{\parallel}$  around the axis parallel to the spin magnetic moments in the crystal. The combination of this  $C_{\parallel}$  symmetry with their  $C_{2\perp}\mathcal{T}$  symmetry, where  $C_{2\perp}$  is a  $180^\circ$  spin-space rotation around an axis perpendicular to the collinear magnetic moments, results in a nonrelativistic inversion symmetric band structure, i.e. energy  $E_{\sigma}(\mathbf{k}) = E_{\sigma}(-\mathbf{k})$ .

In ferromagnets and altermagnets (see Fig. 1)  $\mathcal{T}$ -symmetry in the band structure is broken and thus allows for even-parity wave spin polarization. Ferromagnets exhibit net magnetization in direct space and s-wave-like spin-polarization in momentum space. Altermagnets display d, g, or i-wave modulation in the direct space magnetization density that arises from specific spin symmetries of the atomic crystal structure. The specific spin symmetries combine two fold spin rotation with any crystal rotation transformation [1]. In momentum space, the alternating spin polarization takes, correspondingly,

d,g,or i-wave symmetry with 2, 4, or 6 spin unpolarized nodal surfaces [1, 2, 4].

In conventional collinear antiferromagnets, the inversion symmetry of band structures (due to the  $C_{\parallel}$  a  $C_{2\perp}\mathcal{T}$  symmetries) together with  $\mathcal{T}\tau$  symmetry protects the spin degeneracy over the entire Brillouin zone of the nonrelativistic band structure. (In antiferromagnets with combined  $\mathcal{PT}$  symmetry, where  $\mathcal{P}$  is inversion, both the nonrelativistic and relativistic band structures are forced to be Kramers spin-degenerate [36, 37].)

The sought-after odd-parity wave spin polarization is  $\mathcal{T}$ -symmetric. We thus need to preserve the  $\mathcal{T}$ -symmetry while breaking the inversion symmetry of the nonrelativistic band structure. Here, we identify a previously overlooked class of unconventional magnetic crystals which satisfy these symmetry conditions. These unconventional magnetic crystals break inversion symmetry and feature noncollinear exchange fields, which respect  $\mathcal{T}\tau$  symmetry (see middle panel in Fig. 1 and Fig. 2). Akin to conventional antiferromagnets, the  $\mathcal{T}\tau$  symmetry protects the zero net magnetization of the unconventional magnet.

We have identified two types of odd-parity wave spin order, see Fig. 2(d,e). The first type is associated with collinear p-wave spin polarization found in noncollinear coplanar noncentrosymmetric magnets. This phenomenon is facilitated by the combination of  $C_{2\perp}\mathcal{T}$  symmetry in coplanar noncollinear magnetic orderings, with  $\mathcal{T}\tau$  symmetry. The combination implies  $C_{2\perp}$  symmetry in the spin sector, which protects the collinear orientation of the spin polarization in momentum space. The resulting momentum space spin polarization takes the elusive form of an odd-parity p-wave: it is  $\mathcal{T}$  symmetric, i.e. the spin polarization changes sign for opposite wavevectors,  $E_{\sigma}(\mathbf{k}) = E_{-\sigma}(-\mathbf{k})$  (see Fig. 1). Remarkably the collinear p-wave momentum-independent spin-polarization axis in momentum space is perpendicular to the magnetic moments of the crystal, starkly contrasting spin-quantization axis in ferromagnets and altermagnets, which is oriented along the magnetic moments of the crystal (and is protected by the  $C_{\parallel}$  symmetry).

We note that a momentum-independent spin axis can also be realized in 2D relativistic band structures with equal amplitudes of Rashba and Dresselhaus spin-orbit coupling [38]. However, in p-wave magnets, the momentum-independent spin axis is symmetry protected. In contrast, in the relativistic case, it arises from the suppression of momentum-dependent noncollinearity of spins due to fine-tuned values of microscopic electronic-structure parameters.

The second type of odd-parity wave spin order manifests as a noncollinear odd-parity spin texture in momentum space. We identify the odd-parity wave spin texture in noncentrosymmetric magnets with  $\mathcal{T}\tau$  symmetry that are noncoplanar and thus break

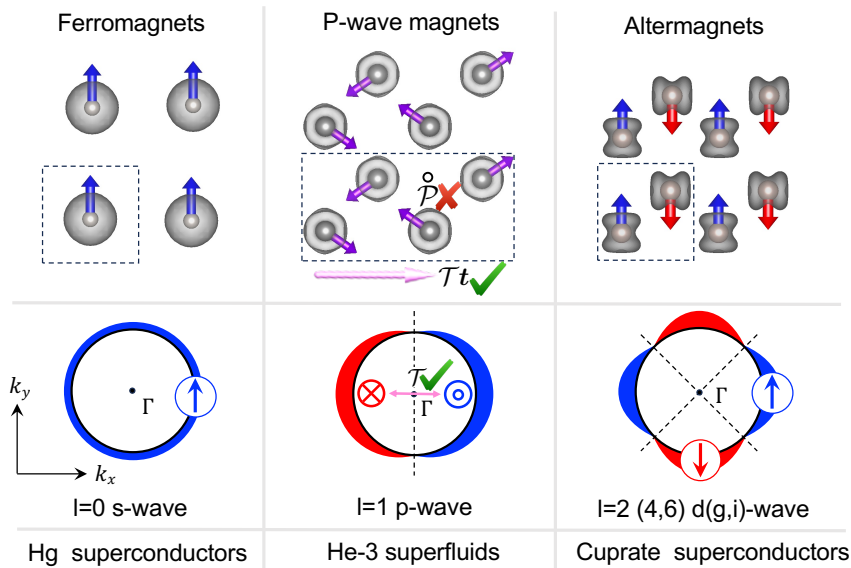


FIG. 1. **Spin symmetry classification of magnets.** The first row shows the magnetic ordering in direct space. The magnetic unit cell is marked by the dashed rectangles. The grey shaded regions are schematic visualisation of the magnetization density around the magnetic atoms. Magenta arrows mark the combined time-reversal and lattice translation symmetry  $\mathcal{Tt}$ . The second row shows schematics of spin polarization in momentum space. We index the spin polarized Fermi surfaces by the angular quantum number  $l = 0, 1, 2, \dots$  corresponding to the number of spin-unpolarized nodal lines/planes (analogous to classification of atomic orbitals). In the p-wave panel we highlight also breaking of inversion symmetry  $\mathcal{P}$  centre marked by the circle, and collinear p-wave spin-polarization which respects time-reversal symmetry  $\mathcal{T}$  and is oriented perpendicular to the direct space magnetic order. Last row lists superconducting or superfluid analogy of magnetic state.

the coplanar  $C_{2\perp}\mathcal{T}$  symmetry. Consequently, this absence of coplanar symmetry leads to a noncollinear odd-parity spin texture in the momentum space. These odd-parity wave spin textures thus represent nonrelativistic unconventional magnetic counterparts to the  $\mathcal{T}$ -symmetric spin textures generated by conventional relativistic spin-orbit coupling [16, 17]. However, their Coulomb-exchange origin brings forward the expectation of generating much larger nonrelativistic spin splittings and associated effects.

### MODEL OF UNCONVENTIONAL ODD-PARITY WAVE SPIN SPLITTING, SPIN POLARIZATION AND SPIN TEXTURE

We now move on to illustrate the proposed unconventional odd-parity wave spin splitting shown in Fig. 2(a). We build a tight-binding model shown in Fig. 2(b). The model comprises a kagome lattice with a noncollinear magnetic ordering which doubles the unit cell spanned by lattice vectors  $\mathbf{a}_1$  and  $\mathbf{a}_2$ . Such a magnetic doubling in a kagome lattice might look artificial, however, below we show that it is experimentally reported in antiperovskite crystals [39].

The model tight binding Hamiltonian reads,

$$H = \sum_i \mathbf{J} \cdot \boldsymbol{\sigma}_i^\dagger c_i + \sum_{\langle ij \rangle} t c_i^\dagger c_j. \quad (1)$$

Here, the first term is the local exchange field at each site whose size and direction are parametrized by  $\mathbf{J}$ , and  $\boldsymbol{\sigma}$  is a vector containing the three spin Pauli matrices. The second term describes nearest-neighbour hopping on the kagome lattice with the hopping amplitude  $t$ . In reciprocal space, the first Brillouin zone is shown by the dashed parallelogram in Fig. 2(c). We consider  $|\mathbf{J}| = t$  and carry out the calculations numerically using the PythTB package version 1.7.2 [40].

The coplanar noncollinear magnetic ordering shown in Fig. 2(b,d) fulfils the above spin symmetry criteria for collinear p-wave spin-polarization. It has the  $C_{2\perp}\mathcal{T}$  and  $\mathcal{T}\tau$  symmetries, and it also breaks the inversion symmetry of the kagome lattice (the inversion center is marked by the black circles in Fig. 2(b)). As seen in Fig. 2(b), the center connects pairs of opposite spins and thus the magnetic order breaks inversion symmetry. The resulting p-wave spin-polarization respects the momentum space  $C_{2\perp}$  symmetry and thus is collinear in momentum space as shown in Fig. 2(d) for the Fermi surface corresponding to energy  $-1.65t$ . However, unlike the spin-polarization in collinear ferromagnets and altermagnets, the spin-polarization is  $\mathcal{T}$  symmetric, and its magnitude is not protected, varying across the Brillouin zone.

Fig. 2(a) shows the corresponding band structure with the computed spin-polarization, and illustrates the linear band splitting dispersion around the  $\Gamma$  point. The

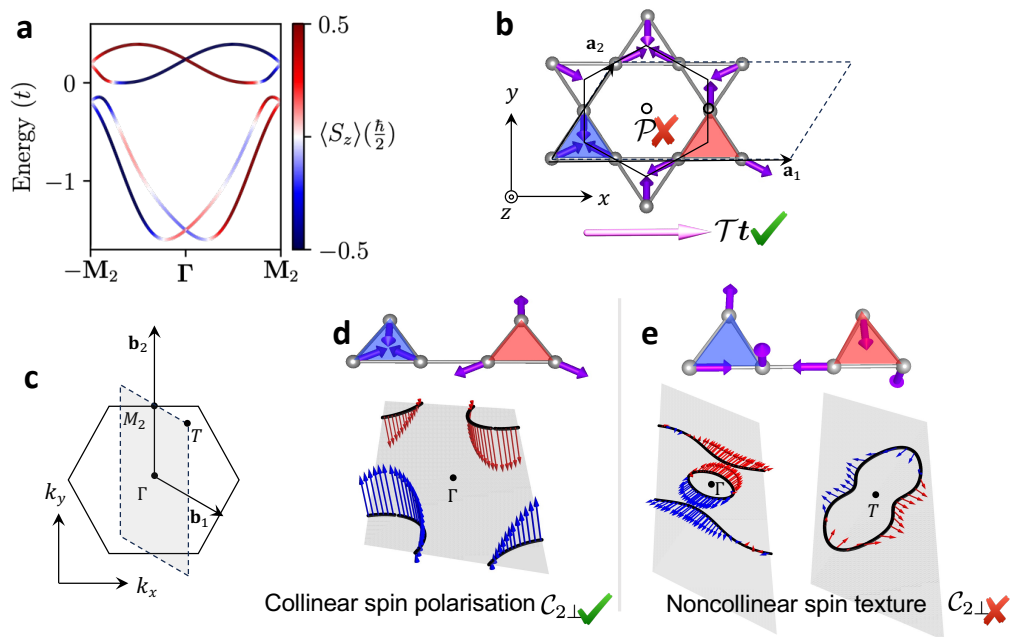


FIG. 2. **Odd-parity-wave exchange spin-splitting, p-wave spin polarization and spin-texture in coplanar and noncoplanar noncollinear double kagome lattice model.** (a) Calculated nonrelativistic odd-parity wave spin-split band structure along the  $-M_2\Gamma M_2$  path with spin projection along out-of-plane direction  $z$ . (b) Direct space magnetic order doubles the kagome lattice unit cell. The magnetic order exhibits combined time-reversal and lattice translation symmetry  $\mathcal{T}t$  marked by the magenta arrow which connects the spins in the blue and red shaded triangles. The magnetic ordering breaks the inversion centre  $\mathcal{P}$  of the kagome lattice marked by the circle. (c) Brillouin zone of the kagome (hexagon) and double kagome (dashed line). (d) The coplanar noncollinear magnetic ordering (top inset) and computed out-of-plane collinear p-wave spin polarization in momentum space respects the  $C_{2\perp}$  symmetry, computed for energy  $=-1.65t$ . (e) The noncoplanar magnetic ordering (top inset) and the computed spin-texture centered at  $\Gamma$  and energy  $=-1.39t$  (left) and centered at  $T$  and energy  $=0.65t$  (right).

bands also reflect the  $\mathcal{T}$  symmetry, i.e., the  $\langle S_z \rangle$  spin polarization, shown in Fig. 2(a), has opposite signs along the opposite paths.

Finally, we consider the noncoplanar magnetic order case, shown in the top inset of Fig. 2(e). It preserves all discussed symmetry criteria for odd-parity wave magnetism but additionally breaks the coplanar  $C_{2\perp}\mathcal{T}$  symmetry. The momentum-dependent spin axes are not forced to be collinear and instead form a noncollinear spin texture as illustrated on the Fermi surface for a Fermi energy of  $-1.39t$  in Fig. 2(e, left). This Fermi-surface spin texture preserves  $\mathcal{T}$  symmetry in momentum space at every wavevector and for all three spin projections, as seen in Fig. 2(e, left). We also show that the coplanar noncollinear spin texture can arise around another time-reversal invariant momentum  $T$  in the Brillouin zone in Fig. 2(e, right) plotted for energy of  $0.65t$ . Here we see that the spins wind once around the Fermi surface, akin to the spin texture arising from relativistic Dresselhaus spin-orbit coupling. However, unlike in the relativistic case, our exchange spin textures are not helically-locked, both their phase and magnitude depend on the wavevector, and lead to strongly anisotropic band structure.

We point out that the coplanarity of the spin texture

in the momentum space is protected by a symmetry of the noncoplanar magnetic order on the crystal combining the  $C_{2z}$  rotation transformation with a spin-space  $C_{2z'}$  rotation transformation (here the spin-space  $z'$ -axis is parallel to one of the three noncoplanar magnetic moments).

The spin polarized band structure for our model noncoplanar magnet has an analogous odd-parity wave form to the coplanar model (see Fig. S1), but has nonzero  $\langle S_x \rangle$  and  $\langle S_y \rangle$  spin projections, and zero  $\langle S_z \rangle$  projection.

We have also verified that when we set the magnetic ordering to be collinear and retain the  $\mathcal{T}\tau$  symmetry, the calculated bands are spin-degenerate in the whole Brillouin zone (see the black bands in Fig. S1).

## AB INITIO THEORY OF MATERIALS

We now demonstrate, based on our symmetry analysis and *ab initio* calculations, realistic material candidates for the odd-parity wave collinear spin-polarization and noncollinear spin-texture in the band structure. We calculate the band structure using the Vienna Ab Initio Simulation Package (VASP), with the Perdew-Burke-Ernzerhof (PBE) exchange-correlation

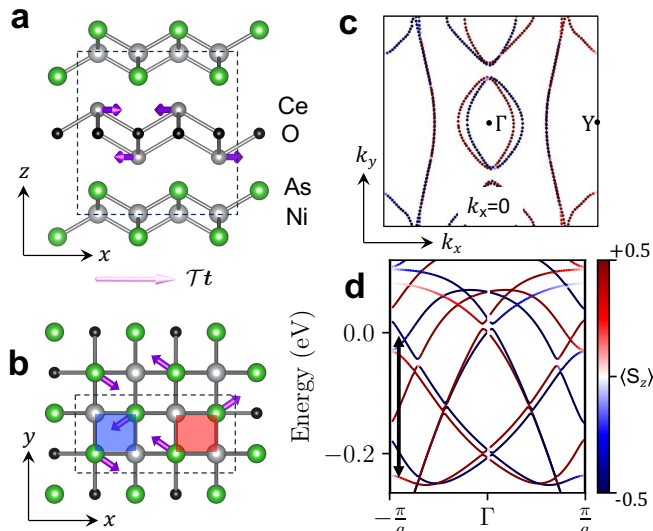


FIG. 3. **Odd-parity p-wave spin polarization calculated from *ab initio* in unconventional noncollinear coplanar magnet CeNiAsO.** (a,b) Side and top view of the magnetic and crystal structure of CeNiAsO with  $\mathcal{T}\tau$  symmetry marked by magenta arrow. (c) Constant energy isosurface in momentum space  $k_z = 0$  plane demonstrates p-wave spin-polarization. (d) Nonrelativistic odd-parity wave spin splitting of energy bands plotted along the  $-X\Gamma X$  path. The spin splitting magnitude reaches  $\sim 200$  meV which is marked by the double arrow.

functionals [41–43], constrained noncollinear magnetism, symmetrization switched off, and in the nonrelativistic limit (without relativistic spin-orbit coupling). To facilitate convergence, we add a penalty potential in the noncollinear magnetic calculations (see Methods for details).

*Material with p-wave spin-polarization* – In the middle panel of Fig. 1 and in Fig. 3(a,b), we show the magnetic and crystal structure of the p-wave candidate compound CeNiAsO. The nonmagnetic unit cell contains two formula units. The crystal structure can be seen as an alternating stacking of quasi-2D layers of O-Ce and Ni-As, with both layers taking the PbO crystal structure (the same crystal structure as FeSe [44]). The experimentally reported magnetic state leads to a doubling of the unit cell as compared to the nonmagnetic phase, i.e., it has the required  $\mathcal{T}\tau$  spin symmetry as marked in Fig. 1 by the magenta arrow (corresponding Type-IV magnetic space group  $P_a2_1$ ). In Fig. 3(b), the  $\mathcal{T}\tau$  symmetry connects the opposite spins in the blue and red squares. The magnetic ordering is coplanar noncollinear and thus respects the  $C_{2\perp}\mathcal{T}$  symmetry. Finally, the magnetic ordering breaks the inversion center of the nonmagnetic crystal structure highlighted by the black circle in the p-wave panel in Fig. 1.

The p-wave Fermi surfaces are shown in Fig. 3(c). We observe several band sheets in Fig. 3(c). The collinear p-

wave spin polarization with anisotropically split Fermi surfaces, can be seen as counterpart of the anisotropic  $^3\text{He-A}$  phase [45]. The band structure is shown in Fig. 3(d) where we observe spin splittings reaching up to 200 meV. The bands spin split linearly in momentum near the  $\Gamma$ -point. The giant values for a  $\mathcal{T}$ -symmetric spin splitting originate from the nonrelativistic exchange.

*Material with odd-parity wave noncollinear spin-texture* – In Fig. 4 we discuss material candidates for the odd-parity wave noncollinear spin-texture in the momentum space within the family of antiperovskite crystals. The cubic lattice of the nonmagnetic antiperovskite crystal structure contains five atoms. We consider the noncoplanar magnetic state which is consistent with our symmetry criteria for odd-parity wave spin texture. The magnetic structure is experimentally reported in antiperovskite  $\text{Ce}_3\text{InN}$  [39] and its tilted version in the M-1 phase of  $\text{Mn}_3\text{GaN}$  [46]. The noncoplanar magnetic order leads to a doubling of the unit cell as compared to the nonmagnetic phase. It has thus the required  $\mathcal{T}\tau$  symmetry corresponding to a type-IV magnetic space group  $P_C42_12$  [39].

Figure 4(a) shows the crystal and magnetic structure in the (201)-plane. Remarkably, in this plane, the noncoplanar magnetic moments form the double kagome structure analogous to our model in Fig. 2(d). For example, the three magnetic atoms in the blue coloured triangle are related to the three atoms in the red coloured triangle by the  $\mathcal{T}\tau$  spin symmetry with  $\tau = (\frac{1}{2}, \frac{1}{2}, -1)$ . The dashed box is the tetragonal unit cell. For the sake of illustrating the noncollinear spin texture in materials containing low atomic number elements, we choose in Fig. 4(b-e) a system with a magnetic sublattice of Ce (atomic number 58) substituted by Mn (atomic number 25) [47]. Except for the values of the lattice parameters, the crystal structures of  $\text{Mn}_3\text{GaN}$  and  $\text{Ce}_3\text{InN}$  are identical [46] and qualitatively our conclusions apply to both crystals (see also Fig. S3 and S4).

Fig. 4(b–d) shows the calculated Fermi surface of  $\text{Mn}_3\text{GaN}$  in the (001)-plane ( $k_z = 0$ ). We observe a spin texture in our calculations akin to the noncoplanar kagome model discussed in Fig. 2(e). The  $\langle S_x \rangle$  component shown in Fig. 4(b) vanishes, while the  $\langle S_y \rangle$  (Fig. 4(c)) and  $\langle S_z \rangle$  (Fig. 4(d)) projections take the odd-parity wave form. The resulting noncollinear spin texture can be seen as composed from two differently oriented collinear p-wave spin polarizations as highlighted schematically by the differently rotated nodal lines which are marked by the dashed lines in Fig. 4(c,d). This noncollinear odd-parity wave spin texture can be seen as counterpart of isotropic  $^3\text{He-B}$  phase [45]. In contrast to the split Fermi surfaces in Fig. 3(d), here the odd-parity wave symmetry in the spin sector is realized on a single principally isotropic Fermi surface.

Finally, we demonstrate the large scale of the spin splitting induced by the nonrelativistic noncoplanar p-

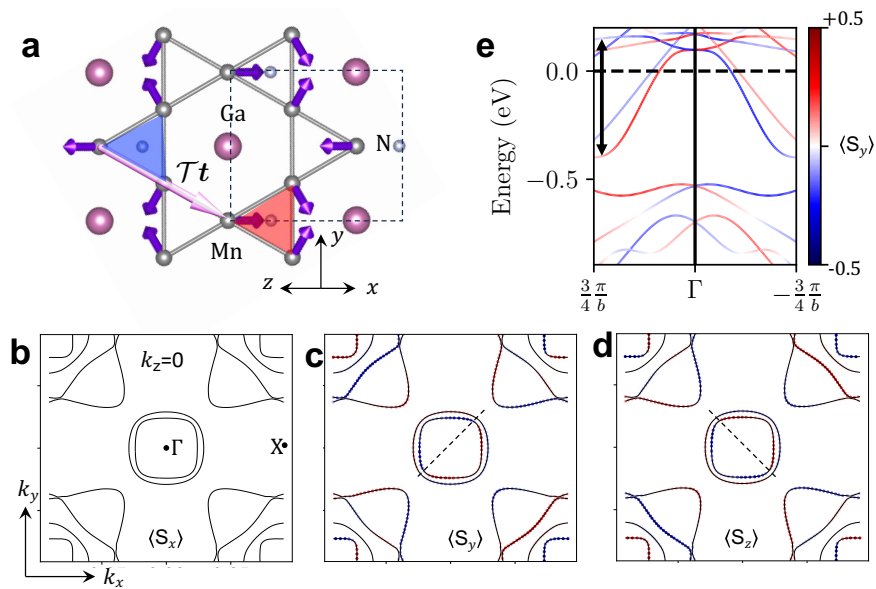


FIG. 4. **Odd-parity-wave spin-texture calculated from *ab initio* in unconventional noncoplanar magnet  $\text{Mn}_3\text{GaN}$ .** (a) The crystal structure of  $\text{Mn}_3\text{GaN}$  (and  $\text{Ce}_3\text{InN}$  and) in the (201)-plane with magnetic moments indicated by red arrows. The crystal forms a kagome lattice with  $\mathcal{T}\tau$  spin symmetry, where the translation  $\tau$  is shown by the light magenta arrow. (b-d) (left) The computed Fermi surface and spin-polarization for  $\text{Mn}_3\text{GaN}$  along  $x$ ,  $y$ , and  $z$  directions respectively. The red and blue colouring indicates the positive and negative spin polarization value. (e) *Ab initio* calculations showing spin split energy bands with  $\mathcal{T}$  symmetry and spin polarization  $\langle S_y \rangle$ . The double arrow marks large 0.5 eV spin splitting around Fermi level in this low atomic number compound.

exchange. In Figs. 4(e) we show the *ab initio* band structure of  $\text{Mn}_3\text{GaN}$ . The bands with spin projections are plotted along the  $k_y$  direction (for more band structures see Supplementary Figs. S3,4). We observe a giant magnitude of the spin splitting reaching  $\approx 500$  meV, as highlighted by double arrows in Fig. 4(e).

Such a large spin splitting is at least 1-2 orders of magnitude stronger than the spin splitting induced by the relativistic spin-orbit coupling in noncentrosymmetric compounds with the same chemistry, and are larger than record spin-orbit coupling induced spin splitting reaching 100 meV in  $\text{BiTeI}$  [48].

## LIST OF MATERIAL CANDIDATES AND DISCUSSION

According to our symmetry-derived rules, we have identified numerous noncollinear noncentrosymmetric magnets with the  $\mathcal{T}\tau$  symmetry. Additionally to the above-studied  $\text{CeNiAsO}$  and  $\text{Mn}_3\text{GaN}$ , we found 58 additional candidates in the Magndata database [49] (listed in supplementary Tab. S1). Among these, 45 are coplanar, exhibiting collinear p-wave spin-polarization in the momentum space. Remarkably, the list includes the low atomic number compound  $\text{Mn}_5\text{Si}_3$ . In supplementary Fig. S5, we present a noncollinear noncentrosymmetric magnetic structure with  $\mathcal{T}\tau$  symmetry, likely realized close to the transition from a high-temperature collinear

to a low-temperature noncollinear phase in bulk  $\text{Mn}_5\text{Si}_3$  [50, 51]. The computed band structure in Fig. S5 showcases an odd-parity wave exchange spin-splitting, potentially contributing to the reported sensitivity of the material to magnetic fields and to its unconventional magnetotransport properties [50–52].

We point out that the 60 materials with nonrelativistic spin split band structures identified in our work, were missed in prior studies [12, 13, 53] because of the expressed misconception [12–14, 53] that it is impossible to realize a nonrelativistic spin splitting in compensated magnets with opposite spin sublattices related by lattice translation (magnets with the type-IV magnetic space groups). It is impossible to achieve nonrelativistic spin splitting only in the collinear subset of  $\mathcal{T}\tau$  symmetric magnets because they exhibit centrosymmetric bands independently whether the magnetic crystal is or is not centrosymmetric. That is perhaps among the reasons why p-wave magnets were also impossible to realize in the past [10, 25, 26]. Here we also point out that our  $\mathcal{T}$  symmetric nonrelativistic odd-parity wave spin polarization and spin texture are principally distinct from the even parity wave noncollinear spin textures in the band structure of  $\text{Mn}_3\text{Sn}$ -like noncollinear (see supplementary Fig. S6 [54, 55]), multipolar [56, 57] and also noncoplanar orderings [14, 58, 59] studied in magnetic crystals that do not have the  $\mathcal{T}\tau$  symmetry.

Our identification of p-wave magnetism, based on

nonrelativistic spin symmetries of crystals with a noncollinear magnetic order, is conceptually different from previous unsuccessful attempts to realize p-wave magnetism via strongly correlated instabilities [10, 25, 26] and hidden orders [60]. Unlike correlated metallic electron fluids [61], and alike altermagnetism, our spin symmetry based approach allows p-wave magnetism to materialize even at the single quasi-particle level of density functional theory. As a result, our p-wave magnetism opens the possibility of its robust material realization, direct photoemission observation and device exploitation in metallic and insulating phases.

To conclude, we have identified the analogy of superfluid  $^3\text{He}$  in unconventional odd-parity wave magnetism, which has been elusive for many decades [10, 11]. While in our unconventional p-wave magnetism we consider the ordering of electrons in the spin channel, in superfluidity [8] the ordering corresponds to the p-wave Cooper pairing of the fermionic  $^3\text{He}$  atoms [9]. The superfluid  $^3\text{He}$  is known to host a plethora of rich and anisotropic properties. In turn, similarly intriguing physics can now emerge in p-wave magnets. P-wave spin currents are an example of extraordinary phenomena anticipated in the p-wave magnets [11]. Attractive properties of p-wave magnets are the giant magnitude of odd-parity wave exchange spin splittings, strongly anisotropic band structure, collinear p-wave spin polarization and the possibility to control the spin-polarization by manipulating the direct-space magnetic order. The linear p-wave dispersion around the  $\Gamma$ -point akin to relativistic spin-orbit coupled band structures is also a promising feature to be explored in the context of topological quasi-particles [19, 21].

## ACKNOWLEDGMENTS

We acknowledge fruitful discussions with Jörg Schmalian, Rafael M. Fernandes, Andrey Chubukov, Rafael González Hernández, Rodrigo Jaeschke Ubierno, and Nayra Alvarez. We acknowledge funding from the Czech Science Foundation Grant No. 19-18623X, the Ministry of Education of the Czech Republic Grants No. LM2018096, LM2018110, LM2018140, and LNSM-LNSpin, CZ.02.01.01/00/22008/0004594, ERC Advanced Grant no. 101095925, Deutsche Forschungsgemeinschaft Grant TRR 173 268565370 (project A03) and TRR 288 42221347 (project B05), the Johannes Gutenberg University Grant TopDyn, and the computing time granted on the supercomputer Mogan at Johannes Gutenberg University Mainz (hpc.uni-mainz.de).

- [1] L. Šmejkal, J. Sinova, and T. Jungwirth, *Physical Review X* **12**, 031042 (2022).
- [2] L. Šmejkal, J. Sinova, and T. Jungwirth, *Physical Review X* **12**, 040501 (2022).
- [3] I. Mazin, *Physical Review X* **12**, 040002 (2022).
- [4] L. Šmejkal, R. González-Hernández, T. Jungwirth, and J. Sinova, *Science Advances* **6**, eaaz8809 (2020).
- [5] J. Krempaský, L. Šmejkal, S. W. D'Souza, M. Hajlaoui, G. Springholz, K. Uhlířová, F. Alarab, P. C. Constantinou, V. Strocov, D. Usanov, W. R. Pudelko, R. González-Hernández, A. B. Hellenes, Z. Jansa, H. Reichlová, Z. Šobáň, R. D. G. Betancourt, P. Wadley, J. Sinova, D. Krieger, J. Minár, J. H. Dil, and T. Jungwirth, *Nature* **626**, 517 (2024).
- [6] O. Fedchenko, J. Minar, A. Akashdeep, S. W. D'Souza, D. Vasilyev, O. Tkach, L. Odenbreit, Q. L. Nguyen, D. Kutnyakhov, N. Wind, L. Wenthaus, M. Scholz, K. Rossnagel, M. Hoesch, M. Aeschlimann, B. Stadtmueller, M. Klauui, G. Schoenhense, G. Jakob, T. Jungwirth, L. Šmejkal, J. Sinova, and H. J. Elmers, *Science Advances* **10**, 31 (2024).
- [7] S. Lee, S. Lee, S. Jung, J. Jung, D. Kim, Y. Lee, B. Seok, J. Kim, B. G. Park, L. Šmejkal, C.-J. Kang, and C. Kim, *Physical Review Letters* **132**, 036702 (2024).
- [8] A. J. Leggett, *Reviews of Modern Physics* **47**, 331 (1975).
- [9] D. Vollhardt and P. Woelfle, *The Superfluid Phases Of Helium 3*, reprint ed ed. (CRC Press, 2003) p. 656.
- [10] J. E. Hirsch, *Physical Review B* **41**, 6820 (1990).
- [11] C. Wu and S. C. Zhang, *Physical Review Letters* **93** (2004), 10.1103/PhysRevLett.93.036403.
- [12] S. A. Egorov, D. B. Litvin, and R. A. Evarestov, *The Journal of Physical Chemistry C*, acs.jpcc.1c02653 (2021).
- [13] P.-J. Guo, Z.-X. Liu, and Z.-Y. Lu, *npj Computational Materials* **9**, 70 (2023).
- [14] Y.-P. Zhu, X. Chen, X.-R. Liu, Y. Liu, P. Liu, H. Zha, G. Qu, C. Hong, J. Li, Z. Jiang, X.-M. Ma, Y.-J. Hao, M.-Y. Zhu, W. Liu, M. Zeng, S. Jayaram, M. Lenger, J. Ding, S. Mo, K. Tanaka, M. Arita, Z. Liu, M. Ye, D. Shen, J. Wrachtrup, Y. Huang, R.-H. He, S. Qiao, Q. Liu, and C. Liu, *Nature* **626**, 523 (2024).
- [15] C. Autieri, “New type of magnetism splits from convention,” (2024).
- [16] J. Sinova, S. O. Valenzuela, J. Wunderlich, C. Back, and T. Jungwirth, *Reviews of Modern Physics* **87**, 1213 (2015).
- [17] A. Manchon, H. C. Koo, J. Nitta, S. M. Frolov, and R. A. Duine, *Nature Materials* **14**, 871 (2015).
- [18] Y. Tokura, M. Kawasaki, and N. Nagaosa, *Nature Physics* **13**, 1056 (2017).
- [19] L. Šmejkal, Y. Mokrousov, B. Yan, and A. H. MacDonald, *Nature Physics* **14**, 242 (2018).
- [20] A. Manchon, J. Železný, I. M. Miron, T. Jungwirth, J. Sinova, A. Thiaville, K. Garello, and P. Gambardella, *Reviews of Modern Physics* **91**, 035004 (2019).
- [21] B. A. Bernevig, C. Felser, and H. Beidenkopf, *Nature* **603**, 41 (2022).
- [22] P. Strange, *Relativistic Quantum Mechanics*, 1st ed. (Cambridge University Press, 1998) p. 612.
- [23] K. V. Shanavas, Z. S. Popović, and S. Satpathy, *Physical Review B* **90**, 165108 (2014).

- [24] S. Hayami, *Physical Review B* **105**, 024413 (2022).
- [25] E. I. Kiselev, M. S. Scheurer, P. Wölfle, and J. Schmalian, *Physical Review B* **95**, 125122 (2017).
- [26] Y.-M. Wu, A. Klein, and A. V. Chubukov, *Physical Review B* **97**, 165101 (2018).
- [27] L. Šmejkal, A. B. Hellenes, R. González-Hernández, J. Sinova, and T. Jungwirth, *Physical Review X* **12**, 011028 (2022).
- [28] I. I. Mazin, K. Koepf, M. D. Johannes, R. González-Hernández, and L. Šmejkal, *Proceedings of the National Academy of Sciences* **118**, e2108924118 (2021).
- [29] Z. Feng, X. Zhou, L. Šmejkal, L. Wu, Z. Zhu, H. Guo, R. González-Hernández, X. Wang, H. Yan, P. Qin, X. Zhang, H. Wu, H. Chen, Z. Meng, L. Liu, Z. Xia, J. Sinova, T. Jungwirth, and Z. Liu, *Nature Electronics* **5**, 735 (2022).
- [30] R. González-Hernández, L. Šmejkal, K. Výborný, Y. Yahagi, J. Sinova, T. Jungwirth, and J. Železný, *Physical Review Letters* **126**, 127701 (2021).
- [31] R. D. G. Betancourt, J. Zubáč, R. Gonzalez-Hernandez, K. Geishendorf, Z. Šobáň, G. Springholz, K. Olejník, L. Šmejkal, J. Sinova, T. Jungwirth, S. T. B. Goennenwein, A. Thomas, H. Reichlová, J. Železný, and D. Kriegner, *Physical Review Letters* **130**, 036702 (2023).
- [32] A. Bose, N. J. Schreiber, R. Jain, D. fu Shao, H. P. Nair, J. Sun, X. S. Zhang, D. A. Muller, E. Y. Tsymbal, D. G. Schlom, and D. C. Ralph, *Nature Electronics* **5**, 267 (2022).
- [33] H. Bai, L. Han, X. Y. Feng, Y. J. Zhou, R. X. Su, Q. Wang, L. Y. Liao, W. X. Zhu, X. Z. Chen, F. Pan, X. L. Fan, and C. Song, *Physical Review Letters* **128**, 197202 (2022).
- [34] S. Karube, T. Tanaka, D. Sugawara, N. Kadoguchi, M. Kohda, and J. Nitta, *Physical Review Letters* **129**, 137201 (2022).
- [35] I. I. Mazin, *Physical Review B* **107**, L100418 (2023).
- [36] C. J. Bradley and A. P. Cracknell, *The Mathematical Theory of Symmetry in Solids* (Oxford Univeristy Press, 1972).
- [37] L. Šmejkal, J. Železný, J. Sinova, and T. Jungwirth, *Physical Review Letters* **118**, 106402 (2017).
- [38] B. A. Bernevig, J. Orenstein, and S. C. Zhang, *Physical Review Letters* **97**, 236601 (2006).
- [39] F. Gäbler, W. Schnelle, A. Senyshyn, and R. Niewa, *Solid State Sciences* **10**, 1910 (2008).
- [40] D. Vanderbilt, “The pythtb package,” (Cambridge University Press, 2018) pp. 327–362.
- [41] G. Kresse and D. Joubert, *Physical Review B* **59**, 1758 (1999).
- [42] P. E. Blöchl, *Physical Review B* **50**, 17953 (1994).
- [43] J. P. Perdew, K. Burke, and M. Ernzerhof, *Physical Review Letters* **77**, 3865 (1996).
- [44] I. Mazin, R. González-Hernández, and L. Šmejkal, **2**, 1 (2023).
- [45] C. Wu, K. Sun, E. Fradkin, and S.-C. Zhang, *Physical Review B* **75**, 115103 (2007).
- [46] K. Shi, Y. Sun, J. Yan, S. Deng, L. Wang, H. Wu, P. Hu, H. Lu, M. I. Malik, Q. Huang, and C. Wang, *Advanced Materials* **28**, 3761 (2016).
- [47] H. K. Singh, I. Samathrakris, N. M. Fortunato, J. Zemen, C. Shen, O. Gutfleisch, and H. Zhang, *npj Computational Materials* **7**, 98 (2021).
- [48] K. Ishizaka, M. S. Bahramy, H. Murakawa, M. Sakano, T. Shimojima, T. Sonobe, K. Koizumi, S. Shin, H. Miyahara, A. Kimura, K. Miyamoto, T. Okuda, H. Namatame, M. Taniguchi, R. Arita, N. Nagaosa, K. Kobayashi, Y. Murakami, R. Kumai, Y. Kaneko, Y. Onose, and Y. Tokura, *Nature Materials* **10**, 521 (2011), 10.1038/nmat3051.
- [49] S. V. Gallego, J. M. Perez-Mato, L. Elcoro, E. S. Tasci, R. M. Hanson, M. I. Aroyo, G. Madariaga, J. M. Perez-Mato, L. Elcoro, E. S. Tasci, R. M. Hanson, M. I. Aroyo, and G. Madariaga, *J. Appl. Cryst* **49**, 1941 (2016).
- [50] N. Biniskos, F. J. D. Santos, K. Schmalzl, S. Raymond, M. D. S. Dias, J. Persson, N. Marzari, S. Blügel, S. Lounis, and T. Brückel, *Physical Review B* **105**, 104404 (2022).
- [51] C. Sürgers, G. Fischer, P. Winkel, and H. V. Löhneysen, *Nature Communications* **5**, 3400 (2014).
- [52] H. Reichlova, R. Schlitz, and S. T. B. Goennenwein, *Physics* **13**, 83 (2020).
- [53] L.-D. Yuan, Z. Wang, J.-W. Luo, and A. Zunger, *Physical Review Materials* **5**, 014409 (2021).
- [54] J. Železný, Y. Zhang, C. Felser, and B. Yan, *Physical Review Letters* **119**, 187204 (2017).
- [55] L. Šmejkal, A. H. MacDonald, J. Sinova, S. Nakatsuji, and T. Jungwirth, *Nature Reviews Materials* **7**, 482 (2022).
- [56] S. Hayami, Y. Yanagi, and H. Kusunose, *Physical Review B* **101**, 220403 (2020).
- [57] S. Hayami, Y. Yanagi, and H. Kusunose, *Physical Review B* **102**, 144441 (2020).
- [58] R. Shindou and N. Nagaosa, *Physical Review Letters* **87**, 116801 (2001).
- [59] W. Feng, J.-P. Hanke, X. Zhou, G.-Y. Guo, S. Blügel, Y. Mokrousov, and Y. Yao, *Nature Communications* **11**, 118 (2020).
- [60] W. Knafo, S. Araki, G. Lapertot, D. Aoki, G. Knebel, and D. Braithwaite, *Nature Physics* **16**, 942 (2020).
- [61] E. Fradkin, S. A. Kivelson, M. J. Lawler, J. P. Eisenstein, and A. P. Mackenzie, *Annual Review of Condensed Matter Physics* **1**, 153 (2010).